Received: 8 February 2022 | Revised: 9 April 2023 | Accepted: 24 April 2023

DOI: 10.1002/dep2.233

The Depositional Record Open Access
A journal of the International Association of Sedimentologists
WILEY

ORIGINAL RESEARCH ARTICLE

The effect of sea-level rise on estuary filling in scaled landscape experiments

Steven A. H. Weisscher | **Pelle H. Adema** | **Jan-Eike Rossius** | **Maarten G. Kleinhans**

Faculty of Geosciences, Department of Physical Geography, Utrecht University, Utrecht, The Netherlands

Correspondence
Steven A. H. Weisscher, Faculty of Geosciences, Department of Physical Geography, Utrecht University, Princetonlaan 8A, 3584 CB, Utrecht, The Netherlands.
Email: steven@weisscher.nl

Funding information
H2020 European Research Council, Grant/Award Number: 647570

Abstract

When sea-level rise slowed down in the middle Holocene, fluvial and coastal sediments filled the newly created accommodation, whilst others remained largely unfilled because of limited sediment supply. In view of current and future rapid sea-level rise, the question arises how estuarine systems will adapt and whether the land-level rise may keep up. Besides geological data and conceptual models of large-scale and long-term estuary filling, little is known about the filling process during sea-level rise on the decadal-to-centennial time scale that is relevant for society. This study focusses on how sea-level rise affects the morphological and hydrodynamic development of filling estuaries. To this end, scaled laboratory experiments were conducted in a tilting flume facility that creates bidirectional tidal currents and develops entire estuaries. A net importing estuary with sand, mud and vegetation was formed that was subjected to linear sea-level rise. Findings show less of the imported sand was deposited landward following sea-level rise than in an experiment without sea-level rise. The bay-head delta and the flood-tidal delta retained nearly enough sediment to keep up with sea-level rise, whilst the tidal embayment in between drowned except for the highest vegetated bars. Sea-level rise also reduced vegetation survival and sprouting potential, as prolonged inundation increased mortality, negating the potential eco-engineering effect. This resulted in lower vegetation coverage with sea-level rise than under constant sea level. These findings suggest that sea-level rise may cause natural systems to drown even if nearly sufficient sediment is available to fill the newly created accommodation, particularly in areas further away from the fluvial and marine sediment sources. Finally, depending on the sea-level rise rate, the flood-tidal delta may show back-stepping like fluvial deltas, but in the reverse direction towards the sea.

KEYWORDS
eco-engineering, estuary, estuary infilling, scaled laboratory experiments, sea-level rise

1 | INTRODUCTION

During the Middle Holocene, many coastal regions drowned in response to rapid sea-level rise, which produced many estuaries around the world (Hijma & Cohen, 2010; Job et al., 2021; Shi & Lamb, 1991; Vos, 2015). Here, an 'estuary' is considered a drowned valley system with both fluvial and marine sediment input and lithofacies influenced by the relative importance of the rivers, waves and tides (cf. Dalrymple et al., 1992). This '(tidal) system' encompasses the tidal morphodynamics that are characteristic of estuaries and is bounded by other systems with fundamentally different processes, that is, a fluvial-dominated river upstream, a mostly wave-dominated spit or barrier coast on the downstream boundary, and continental processes beyond the outer banks. In case of wave-dominated estuaries, the system extends from the upstream limit of tidal influence to the barrier and the ebb-tidal delta downstream (cf. Dalrymple et al., 1992). This differs from a geological 'system', which signifies the entire depositional environment ranging from fluvial deposits upstream to delta toe-sets downstream.

In response to sea-level rise levelling off in the Late Holocene, many estuaries faced a balance shift from net accommodation creation to net estuary filling (Roy et al., 1980). The ongoing delivery of fluvial and marine sediments filled accommodation, which generally resulted in shallower and narrower estuaries (De Haas et al., 2018; Roy et al., 1980). Current conceptual models of how accommodation in estuaries is filled (Dalrymple et al., 1992; Nichol, 1991; Roy et al., 1980) are mainly inferred from the depositional record and focus on (multi)-millennial timescales. These qualitative models allow for the spatial and temporal analysis of large-scale lithofacies distributions in estuaries. Yet, the conceptual models are not detailed enough to shed light on the development of individual tidal channels and intertidal bars and how these geomorphological units respond to sea-level rise and fall on a timescale of decades to centuries. Such small spatial and temporal scales are of high societal relevance in terms of, for example, shipping and flood risk management. Furthermore, effects of sea-level rise on river deltas are much better known from modelling (Elmilady et al., 2022; Guo et al., 2022; van der Wegen, 2013), reconstruction and experiments than for estuaries (see for review De Haas et al., 2018). Therefore, there is a need to improve our understanding on the effect of sea-level rise on estuarine morphology on a spatial scale of individual tidal channels and intertidal bars on a temporal scale of decades to centuries.

1.1 | Filling of Holocene wave-dominated estuaries

Field observations and palaeogeographical reconstructions were employed as an aid to understand how sea-level rise will affect estuaries. Such field data provide insight in the recent, Holocene development of wave-dominated estuaries and in how the balance between the creation and filling of accommodation shapes estuaries.

A well-studied example of the Holocene development of wave-dominated estuaries is the Old Rhine Estuary along the Dutch coast. This estuary exhibited the filling of accommodation while rapid sea-level rise started to level off in the Middle-to-Late Holocene (De Haas et al., 2018; Vos, 2015; Figure 1). Following the drowning of its Pleistocene river valley in the Middle Holocene (Figure 1A,B), the wave-dominated Old Rhine Estuary comprised extensive intertidal flats, bounded downstream by barrier islands and bounded upstream by salt marshes, reed marshes and a small bay-head delta. Further levelling off of the sea-level rise between 6,000 yr BP and 5,000 yr BP caused a shift from a phase of net accommodation creation to net accommodation filling (De Haas et al., 2018; Van der & Beets, 1992). In other words, net sediment delivery and retention outpaced the accommodation created by sea-level rise. At first, sand was deposited within the tidal channels and along the tidal channels as levees, protruding further into the estuary over time. Meanwhile, mud was deposited as mudflats extending from the banks and on high intertidal bars, which reduced the lateral migration of the tidal channels. Vast reed marshes covered the banks of the estuary and expanded laterally into the estuary (Figure 1C). Continued mud deposition and reed expansion contributed to a much narrower estuary (Figure 1C,D). Final closure and filling of the estuary occurred after an avulsion of the River Old Rhine around 3,275 yr BP (De Haas et al., 2019; Roep & Van Regteren Altena, 1988).

This and similar reconstructions of wave-dominated estuaries along the Dutch coast (De Haas et al., 2018; Pierik, 2021; Vos, 2015) highlight the importance of mud and vegetation in the filling of estuaries on a millennial timescale. Furthermore, the case of the Old Rhine Estuary illustrates the necessity of a river inflow that ensures the estuary mouth remains open. This open connection to the sea allowed for incoming tides. On the North Sea, the tide is flood-dominant and brings in sediment from longshore drift and from the shallow sea floor into the estuary (Van der Molen & De Swart, 2001). This is thought to have enabled most Dutch estuaries to at least partially keep up with sea-level rise, by filling part of the newly created accommodation due to sea-level rise (De Haas et al., 2018).

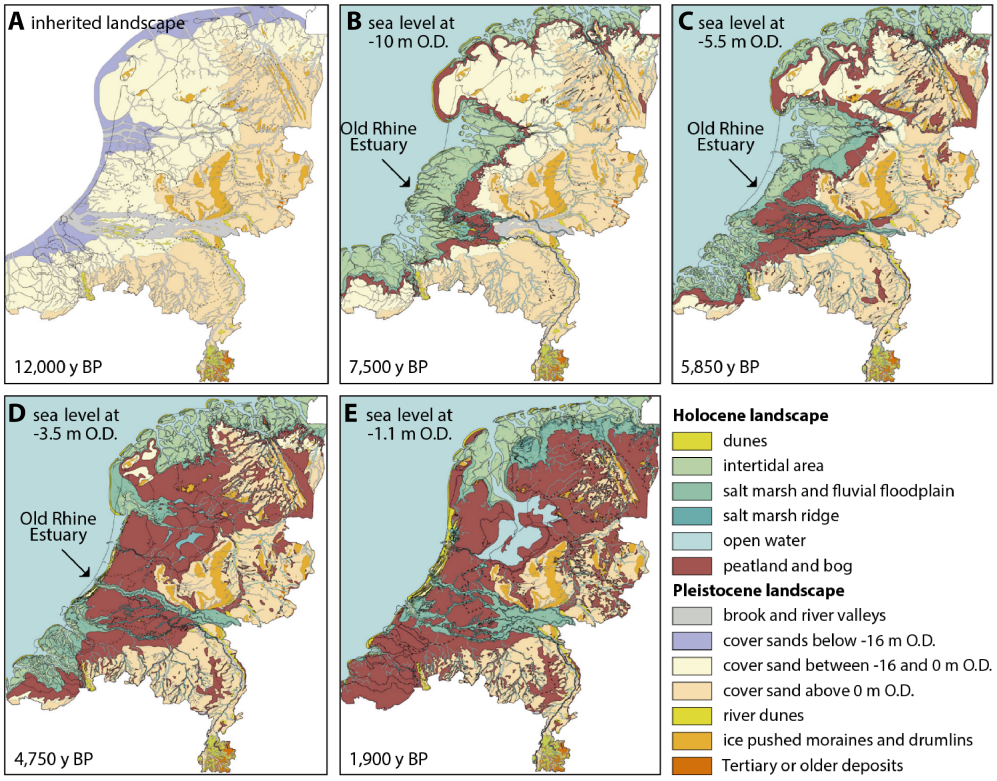

FIGURE 1 Evolution of the Dutch landscape from 12,000 BP to 500 BP. Modified from Vos et al. (2018).

Whilst many estuaries such as the Old Rhine Estuary had their accommodation completely filled and were either closed off from the sea or transfigured into river deltas, there are still estuaries with their accommodation only partly filled or completely unfilled. On the one hand, these systems may have received insufficient sediment supply to fill the available accommodation (Dalrymple & Choi, 2007; De Haas et al., 2018; Lanzoni & Seminara, 2002). On the other hand, over the past few centuries, estuaries such as Arcachon Bay (Allard et al., 2009; Féniès & Faugères, 1998) and Ems-Dollard (Van Maren et al., 2016) remained largely unchanged despite ample sediment supply. This observation suggests that not only boundary conditions such as sediment supply influence the filling of accommodation in estuaries (Clement et al., 2017), but also internal processes that distribute and trap sediment within an estuary (De Haas et al., 2018; Moore et al., 2009). For example, previous studies (Beets & Van der Spek, 2000; De Haas et al., 2018) hypothesised that the development of mudflats and salt marshes plays a key part in storing sediment and confining an estuary. These muddy and vegetated surfaces reduce tidal prism and may increase flood-dominance (Friedrichs, 1995; O'Brien, 1969), which drives further filling of the available accommodation. Yet, this hypothesis is based on the filling of accommodation in an estuary with little sediment supply under negligible sea-level rise. Therefore, it remains unclear to what extent the development of mudflats and salt marshes contribute to the filling of accommodation when sea-level rise is more prominent.

Field data provide ample evidence that estuaries can have their accommodation filled under conditions of mild sea-level rise especially when mud and vegetation are present (Beets & Van der Spek, 2000; De Haas et al., 2018; Pierik, 2021). However, due to the ever-changing boundary conditions and the partial erosion of former deposits, it is challenging to isolate the effect of a single boundary condition (in this case: sea-level rise) on how an estuary develops. Hence, complementary methods of research are necessary in the form of numerical modelling and physical scale experiments.

1.2 | Models and experiments on the filling of accommodation

Numerical modelling and physical scale experiments allow for the isolation of singular boundary conditions (Bokulich & Oreskes, 2017; Oreskes et al., 1994). For instance, numerical models are optimal for sensitivity analysis, yet require parameters for the computation of flow, sediment transport (Baar et al., 2019) and life forms. Alternatively, physical scale experiments use real material with inherent physical laws and make morphological change more tangible, yet come with scale issues that need resolving (Kleinhans et al., 2014a).

Based on previous numerical and experimental studies, the filling of accommodation in estuaries was found to depend on the following initial and boundary conditions and processes. First, sediment is needed to fill an estuary, which is delivered by rivers and may be imported from the sea. Flood-dominant tidal asymmetry ensures that more sediment remains in an estuary and enhances sediment import from the sea (Friedrichs & Aubrey, 1988), contributing to estuary filling (Weisscher et al., 2022). Second, mud and vegetation form mudflats and salt marshes that promote estuary filling. Mud helps fill accommodation, protects the outer banks against erosion and stabilises the positions of channels and bars in numerical models (Braat et al., 2017; Brückner et al., 2021) and experiments (Braat et al., 2019). Vegetation increases the sediment trapping potential and so enhances sediment retention in field observations (Cotton et al., 2006; Stella et al., 2011), numerical models (Brückner et al., 2019, 2021) and experiments (Kleinhans et al., 2022; Tal & Paola, 2007; Weisscher et al., 2022; Zong & Nepf, 2011). Furthermore, vegetation limits flow over bars, resulting in a focus of flow in deeper channels (Luhar et al., 2008; Simon & Collinson, 2002; Stella et al., 2011) that tend to migrate faster (Kleinhans et al., 2022). A combination of mud, poorly sorted sand, vegetation and variations in water discharge (i.e. river floods and tides) was found to form levees and crevasses, which also retain sediment (Boechat Albernaz et al., 2020; Elmilady et al., 2020, 2022). Third, initial and boundary conditions such as inherited topography, subsidence and tidal amplitude at the estuary mouth influence the available accommodation that can be filled (Guo et al., 2021, 2022; Leuven et al., 2019). In turn, the resultant planform shape of the estuary determines the number of channels and bars that can form (Leuven et al., 2018b).

Many numerical models and scale experiments of estuaries assume a constant sea level, so the creation of new accommodation and its influence on estuary morphology on a scale of individual channels and bars are largely untested. An increase in flood storage due to sea-level rise can increase flood dominance and the import of sand from the ebb-tidal delta and adjacent coasts (Du et al., 2018; van der Wegen, 2013). This was found for a back-barrier tidal basin and a similar development may be expected for estuaries. Additionally, Leuven et al. (2019) showed that small estuaries dominated by intertidal bars will likely face rapid sedimentation under sea-level rise, whilst larger estuaries may face sediment starvation and become deeper. How this will impact the individual channels and bars remains underinvestigated, yet is of high societal relevance for shipping fairways and managing flood risk in the coming decades to centuries.

A recent breakthrough in scale experiments allows for the creation of entire estuaries with high enough sediment mobility to produce the ongoing migration of channels and bars as observed in natural estuaries (Kleinhans et al., 2015, 2017b, 2014b). This has opened up new ways of studying estuaries aside from numerical models, which are subject to all the combined errors of sediment transport predictors (Baar et al., 2019). So far, the number of scale experiments of estuaries are limited and focussed, amongst others, on the effects of mud (Braat et al., 2019), vegetation (Kleinhans et al., 2022) and the filling of accommodation (Weisscher et al., 2022). In the latter case, mud and vegetation together enabled bars to grow above the high-water table and these bars point at possible locations where the estuary could keep up with sea-level rise. Sea-level rise remained untested in scale experiments apart from one study (Stefanon et al., 2012), which showed for a back-barrier tidal basin that sea-level rise enlarges the tidal channels and increases their cross-sectional area. Sea-level rise had a negligible effect on the overall channel and bar pattern (i.e. the location and number of channels and bars), but this may be due to the low sea-level rise rate and the low sediment mobility in this experiment. Given the many similarities in tidal characteristics and morphological responses between tidal basins and estuaries, a similar response to sea-level rise is expected for estuaries with limited sediment supply.

1.3 | Objective and hypotheses

The objective is to explore the effects of sea-level rise on the morphological response of a filling estuary. To this end, physical scale experiments were conducted wherein entire estuaries were formed with sand, mud and vegetation on an initially drowned river valley. By design, the experiment was set up to receive slightly less sediment than needed to compensate for new accommodation created by sea-level rise. Hypothetically, this left three possible scenarios of morphological response. First, the entire system may deepen, with subtidal areas rapidly expanding at the expense of intertidal and supratidal areas. Second, parts of the system may aggrade to maintain a stable average depth, whilst other parts further away from a sediment source (i.e. the central part of the estuary) become deeper. Third, the estuary, together with its fluvial and coastal boundaries, may shift upstream. Then, channel and bar patterns will shift upstream, provided there is enough space.

2 | METHODS AND MATERIALS

This study presents the findings of two landscape-scale experiments of estuaries in which the effect of sea-level rise was isolated. The first experiment was a control without

sea-level rise of a filling estuary with sand, mud and live vegetation. This control experiment was also reported in Weisscher et al. (2022), who found that mud alone and vegetation with mud quickened the building and raising of new land compared to an experiment with only sand. The novel, second experiment was a filling estuary with sea-level rise but otherwise the same conditions. Sea-level rise was chosen such that the creation of accommodation slightly outpaced the potential filling of accommodation with fluvial and marine sediments.

2.1 | Flume experiments

The experiments were done in the 'Metronome', a 20 m long and 3 m wide flume that drives tidal currents by periodic tilting over its short central axis (Kleinhans et al., 2017b). This novel tilting method solves a number of scale problems that former experiments with periodic sea-level fluctuations experienced, such as ebb-dominance and very low sediment mobility (Reynolds, 1889; Stefanon et al., 2010, 2012). To date, the tilting setup enabled the development of tidal basins (Kleinhans et al., 2015), ingressive estuaries with sand (Leuven et al., 2018a), mud (Braat et al., 2019), vegetation (Kleinhans et al., 2022), channel dredging (Van Dijk et al., 2021) and infilling estuaries with mud and vegetation (Weisscher et al., 2022).

The initial setting of the experimental estuaries resembled an idealised drowned river valley with an open barrier coast and a long drowned river valley relative to the tidal excursion length (Figure 2), designed to be similar to Weisscher et al. (2022). In a sand bed of 17 m long, 3 m wide and 0.11 m thick, a flat-floored valley, 2.3 m wide by 0.03 m deep, was carved over the full length of the sand bed. The initial sand bed had a median grain size $d_{50} = 0.55$ mm and a coarse tail of $d_{90} = 1.2$ mm to prevent the development of unrealistically large scours (Kleinhans et al., 2017a). The tidal inlet was bordered by two large, sandy barrier islands which were designed to erode over time and act as a source of marine sediment, as alongshore drift was impractical to reproduce in the flume. The flume had an offset tilt of 0.001 m/m, which is a typical fluvial valley slope in landscape experiments (Kleinhans et al., 2014a). A central, straight river channel in the upstream reach of the control experiment had a negligible effect on channelising river flow (Weisscher et al., 2022) and was therefore left out in the new experiment with sea-level rise.

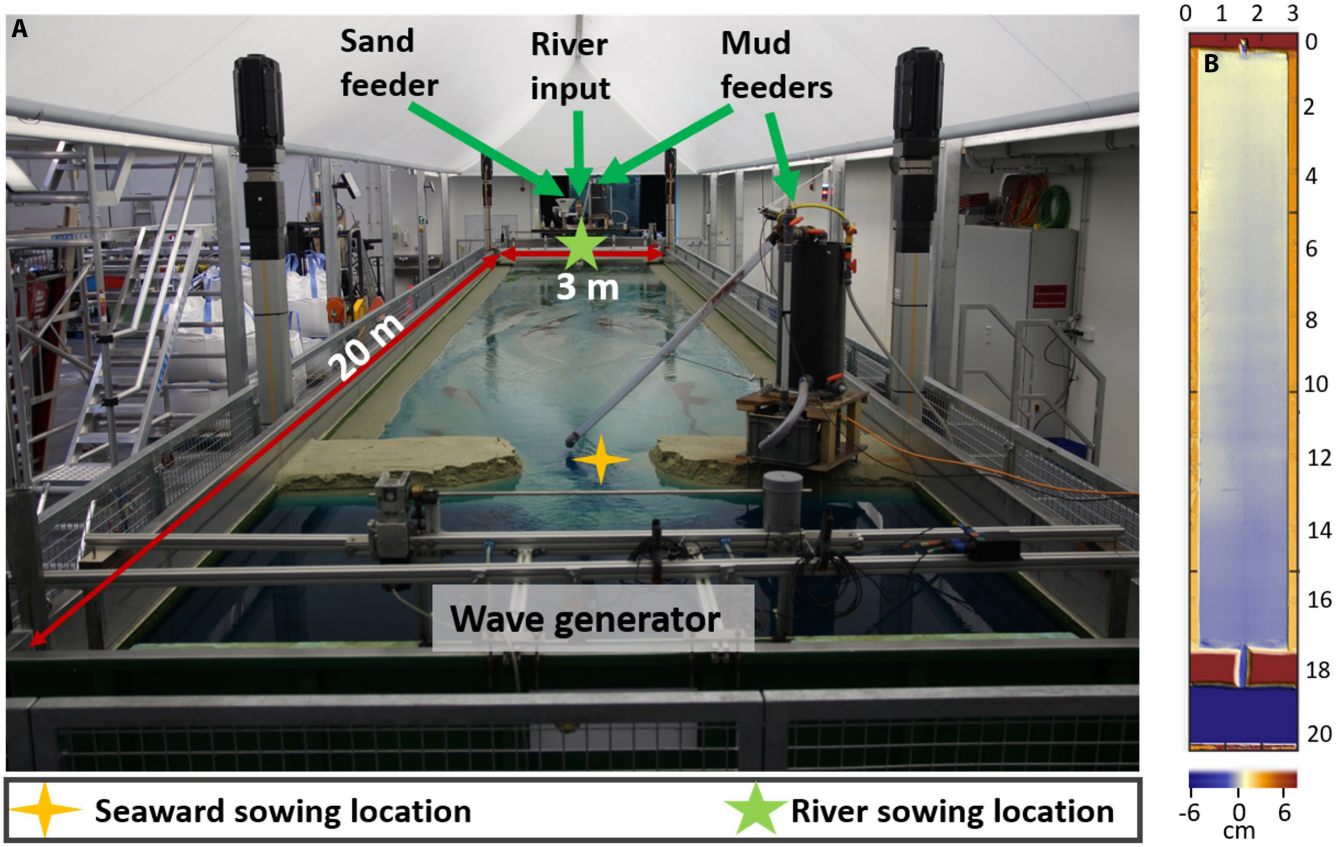

FIGURE 2 (A) Experimental setup of the experiment. The photograph was taken at 2,000 cycles into the sea-level rise experiment. (B) Digital elevation model of the initial bathymetry of the experiment.

The boundary conditions were conducive to filling of the accommodation in the estuary. The flume was tilted with a principal tide of 40 s and an overtide of 20 s for flood dominance. The tilting slope amplitude of the principal tide was 0.0012 m/m and the overtide had an amplitude of 0.006 m/m with a phase difference of 90°. Combined with the initial offset slope of 0.001 m/m, this resulted in a maximum slope of 0.0062 m/m in the upstream direction during flood and 0.0058 m/m in the downstream direction during ebb. At the downstream boundary, a weir moved in the opposite phase of the flume tilting to ensure a constant water head at sea to prevent a water surge during flood and channel incision during ebb. Also, a horizontal paddle generated waves with a frequency of 2 Hz and an amplitude of about 3 mm (for scaling, see supplement to Leuven et al., 2018a). At the upstream boundary, a river discharge of 900 L/h entered the estuary during ebb with a feed of sand and mud, both at a rate 0.4 L/h. Mud was simulated by crushed walnut shell with a density of 1,350 kg/m^3 and a grain size ranging from 0.45 to 1.7 mm, conforming to previous studies (Baumgardner, 2016). Mud was also added at 0.4 L/h at the tidal inlet at the start of every flood to simulate fines from the sea.

Sea-level rise was implemented in the new experiment in 1 mm increments every 1,000 tidal cycles, starting from 3,000 cycles. This culminated in a 7 mm sea-level rise by the end of the experiment at 10,000 cycles, which corresponds to approximately a 12% water depth increase of the 60 mm deep channel at the estuary mouth. Accordingly, a volume of 45 L of accommodation was created every 1,000 cycles, which was by design slightly larger than the total sediment feed (±13 L sand and mud) plus the maximum potential barrier erosion of 25 L per 1,000 cycles. Therefore, based on the filling and creation of accommodation, a slightly transgressive estuary was expected to develop.

2.2 | Seed distribution

Three vegetation species were selected with different eco-engineering effects in a laboratory scale experiment (Lokhorst et al., 2019): *Medicago sativa*, commonly known as alfalfa, *Lotus pedunculatus* and *Veronica beccabunga*. Alfalfa represented riparian vegetation, and *Lotus* and *Veronica* resembled reed-like and grass-like marsh vegetation (Lokhorst et al., 2019).

Seeds were supplied every 500 cycles after an initial 1,000 cycles spin-up, before this point no intertidal area existed where vegetation could establish. The number of seeds was calculated to obtain an average coverage with significant vegetation-induced flow resistance by the end of the experiment at 10,000 cycles, with an average stem density of 0.25 stems/cm^2. In total, 80,000 Alfalfa seeds and 40,000 seeds of both *Lotus* and *Veronica* were supplied to the river and 40,000 seeds of *Lotus* and *Veronica* supplied to the inlet. This amounts to a total of 240,000 seeds on an approximate surface area of 2.4 × 17 m, or a maximum seeding density of 0.59 seeds/cm^2. With a germination probability of 0.5 and a possible fraction of the surface covered by vegetation, say 0.2, this would amount to 1.5 stems/cm^2, about doubling the total flow resistance in vegetated areas compared with the bare bed surface (Lokhorst et al., 2019). Flow resistance of this intensity should be sufficient to affect the partitioning of flow over vegetated and bare areas (Kleinhans et al., 2022). While this is about half the number of seeds of *Lotus* and *Veronica* compared with Weisscher et al. (2022), the actual plant density is mainly limited by air temperature, mould and seed loss by burial, which was controlled better in the second experiment. Moreover, vegetation settling and mortality are mainly determined by inundation duration, which is linked to the degree to which estuary filling can keep up with sea-level rise, and by erosion due to morphodynamics, which is also linked to depth. Increased trapping is less likely in the present setup, which is flood-dominant and captures most sand and mud anyway (Weisscher et al., 2022). As such, vegetation is mainly expected to affect, and be affected by, the pattern and dynamics of the tidal bars.

Each sowing event took 70 tidal cycles to enable distribution of seeds by the flow but avoid most loss, similar to Weisscher et al. (2022). After 10 cycles for initial wetting of the bed following bed scans, pre-soaked seeds were released in the river outlet over 25 cycles. Next, seeds were added just landward of the inlet during the flood phases over the course of 10 cycles, followed by a final 25 cycles to allow the seeds to spread throughout the estuary. The flume was then stopped at its offset slope of 0.001 m/m for 4 days to allow for sprouting before the experiment continued. During sprouting time, the sea was at the current mean sea level and a low 300 L/h river discharge entered the estuary to produce throughflow.

2.3 | Data analysis

Orthophotographs and digital elevation models (DEMs) were made every 1,000 tidal cycles by means of stereophotography of the dry bed. Before shooting stereo photographs with a digital single-lens reflex camera, the Metronome was drained slowly without disturbing the bed. The images were processed in Agisoft Metashape (structure-from-motion software) to create DEMs with a 5 × 5 mm resolution. Most vegetation, apart from dense patches on the bay-head delta, was filtered out using a

low-pass 5% (percentile) filter with a 35 × 35 mm window. To quantify the hydrodynamics, tidal flow was modelled using the numerical model Nays2D (Weisscher et al., 2020) following Weisscher et al. (2022). Nays2D takes as input a DEM and the corresponding boundary conditions and solves the shallow water equations (for review on equations, see Shimizu et al., 2000) as the tilting motion of the flume is reproduced in the model Nays2D. This produces maps of water depth and flow velocity, from which inundation duration and distributions of flow velocity were calculated.

3 | RESULTS

3.1 | General estuary development

The general development of the estuary with sea-level rise resembled that of the constant sea-level experiment in the first 3,000 tidal cycles. At first, short discontinuous tidal channels, separated by low-amplitude bars, formed in the downstream half of the estuary (Figure 3). From this initial low-amplitude, submerged channel and bar pattern, a large flood-tidal delta developed near the tidal inlet together with a small ebb-tidal delta barely extending into the sea. Continued inlet widening by the waves and the incoming tide eroded sediment that was predominantly transported onto the flood-tidal delta. Compared to the experiment with a constant sea level, the upstream half of the estuary in the sea-level rise experiment remained largely unaltered in the first 3,000 tidal cycles, apart from a vegetated bay-head delta forming from the upstream boundary (Figure 4). At first, *Alfalfa* established on the bay-head delta within the first 1,000 tidal cycles, followed by *Lotus* and *Veronica* whose seeds were either germinating slower, captured by existing vegetation or transported to other low-energy regions on the bay-head delta. Shortly after vegetation establishment, a first avulsion occurred on the bay-head delta at 2,000 cycles, resulting in a new main channel with several active branches, similar to the constant sea-level experiment.

After sea-level rise commenced at 3,000 tidal cycles, the focus of sediment deposition remained on the bay-head delta (x = 0–3 m) and the flood-tidal delta (x = 10–17 m) throughout the experiment (Figures 3, 5B and 6). This differed from the constant sea-level experiment, where sediment deposition extended along estuary and resulted in the development of intertidal and supratidal bars along the entire estuary (Figure 3). In the sea-level rise experiment, most fluvial sand and mud was retained and protected by the dense vegetation, whilst most marine sand and mud elevated the flood-tidal delta. Hence, only little sediment was transported further upstream. Upstream transport commenced mainly in the form of lobate bars, or terminal

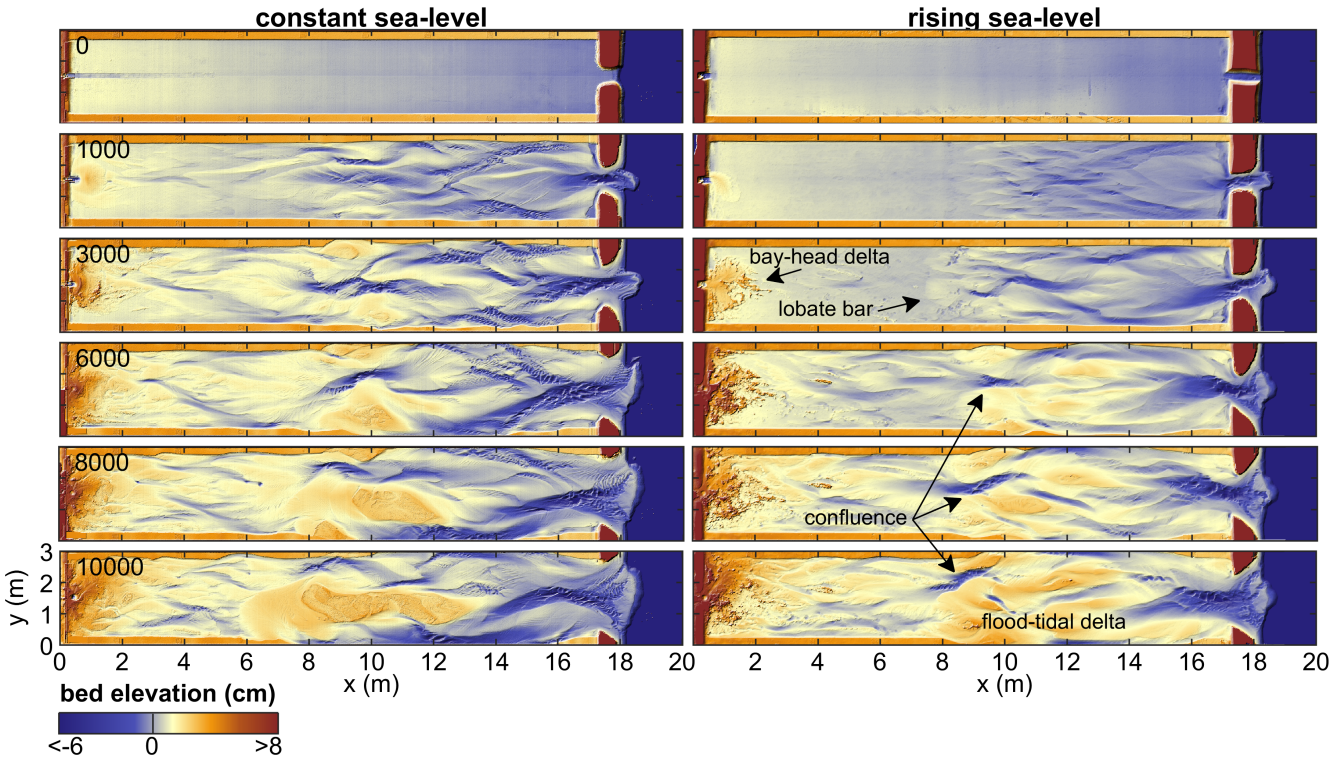

FIGURE 3 Digital elevation models of the experiments with a constant sea level (left column) and with sea-level rise (right column), after 0, 1,000, 3,000, 6,000, 8,000 and 10,000 tidal cycles. Vegetation was excluded from the DEMs.

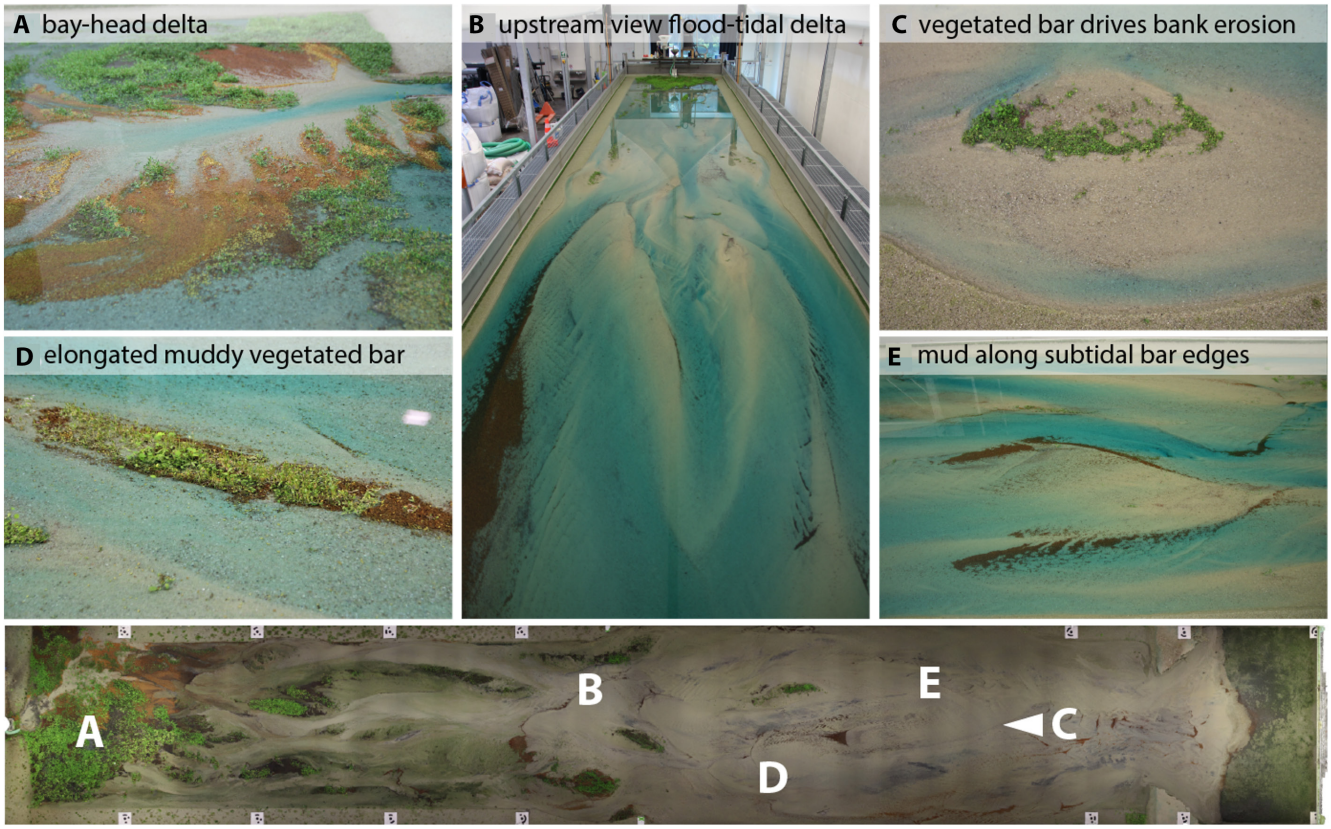

FIGURE 4 Photographs of self-formed features of the experiment. Roman numerals in the orthophotographs correspond to positions of the photographs.

lobes, at the upstream ends of upstream-extending tidal channels (Figure 3, e.g. from 10 to 8 m at 1,000–3,000 cycles), upstream of which the estuary morphology hardly changed. The little sediment imported beyond the flood delta was not nearly enough to avoid the deepening of the initially already deep subtidal bay in the range $x = 3$–8 m (Figures 3 and 7F,H). This region remained largely subtidal until 6,000 cycles (Figure 7D,F). The few intertidal and supratidal areas that formed along the estuary were sparsely colonised by *Lotus* and *Veronica* (Figure 4) and covered with mudflats. Yet, most mud was overridden by migrating sand bars and preserved in the subsurface. Also, prolonged inundation due to sea-level rise caused considerable mortality of the vegetation on the bay-head delta and bar tops. Consequently, after 3,000 tidal cycles of sea-level rise, the intertidal and supratidal area in the central reach of the estuary (from 6 to 14 m) is significantly smaller than in the constant sea-level experiment (Figures 7A through H and 8).

From 6,000 tidal cycles onward, the estuary subjected to sea-level rise developed increasingly more intertidal area. This created new sites for vegetation establishment and mudflat deposition just downstream of the bay-head delta and near the flood-tidal delta (Figure 4). Yet, only very few muddy and vegetated bars elevated into a supratidal elevation reach (Figures 7A through H and 8). Generally, vegetation near the flood-tidal delta seemed sparser and on average younger than near the bay-head delta, suggesting a faster turn-over rate of intertidal vegetation. Also, a large channel confluence formed around $x = 10$ m, which deepened and produced a pulse of sediment further upstream into the deep subtidal bay at $x = 3$–8 m (Figures 3 and 5B). This caused slightly higher bedlevels in the upstream half of the estuary but was largely insufficient to reach an intertidal elevation. In comparison, the estuary with a constant sea level developed a large mid-channel bar covered with abundant vegetation and extensive mudflats.

3.2 | Effect of sea-level rise

Comparison with the constant sea-level experiment shows that sea-level rise impacted the morphological development in the following ways. First, sea-level rise created new accommodation which prompted sediment deposition closer to the tidal inlet (Figures 3 and 6C). Consequently, the bulk of imported marine sediment was transported less far in the upstream direction in the first 6,000 tidal cycles compared to the constant sea-level experiment (compare

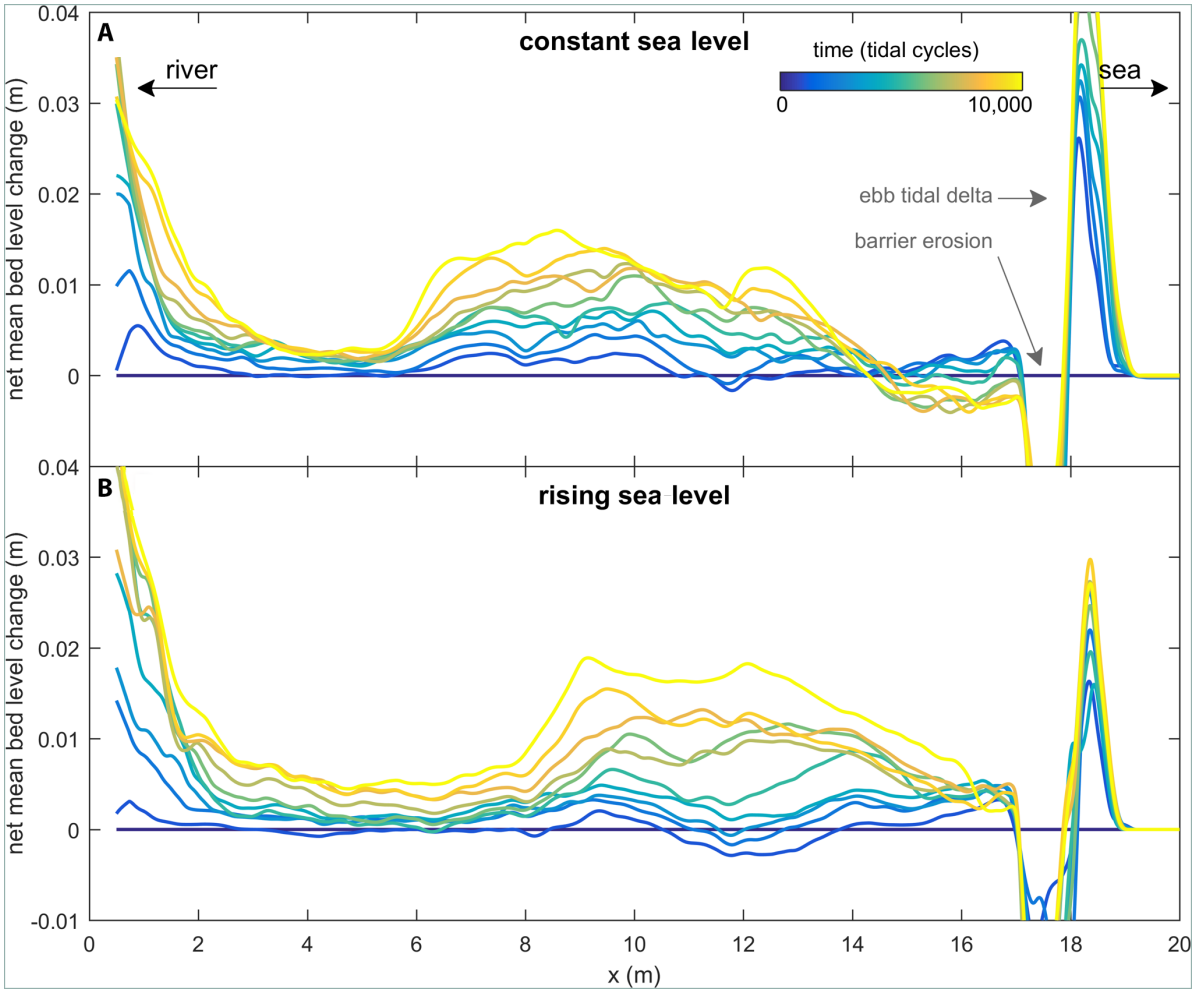

FIGURE 5 Mean bedlevel change (A) along the experiment with constant sea level (Weisscher et al., 2022) and (B) the new experiment with sea-level rise. Calculations exclude the unreworked outer banks of the estuary. Mean bedlevel change is calculated using the initial bathymetry and not relative to the current sea level.

bulk of sediment in the middle-to-downstream part of the estuary in Figures 3 and 6B). Afterwards, the development of a large confluence landward of the flood delta in the sea-level rise experiment scoured bed sediment that was transported towards the subtidal bay. Although this resulted in slightly higher mean bed elevations for the range $x = 3$–8 m in the sea-level rise experiment, the increase in bed elevation was outpaced by sea-level rise. This led to fewer large intertidal and supratidal areas compared with the constant sea-level experiment (Figure 7).

Second, prolonged inundation time (Figure 7) due to sea-level rise increased plant mortality and limited the area suitable for vegetation establishment. Consequently, less vegetation established and survived in the middle of the estuary, concurrent with faster channel migration, which resulted in a net loss of vegetation in the second half of the experiment. In contrast, vegetation on the bayhead delta was more abundant in the sea-level rise experiment. However, this difference could also be due to the poorer control of mould in the experiment without sea-level rise. Regarding the central part of the estuary ($x = 6$–14 m; Figure 8), the intertidal area nearly doubles when the original sea level was imposed on the bathymetry of the sea-level rise experiment. In contrast, the intertidal area hardly changed when the final sea level of the sea-level rise experiment was imposed on the bathymetry of the constant sea-level experiment. One possible explanation for this is that most of the loss in intertidal area was compensated for by the conversion of supratidal to intertidal. Alternatively, the loss of supratidal area under instantaneous sea-level rise was much larger than the gain of supratidal area for the sea-level rise experiment under the original sea level (Figure 8), showing that the central part of the estuary aggraded higher under sea-level rise than under constant sea level, but with less supratidal and vegetated area.

Third, flow velocity was on average larger with less spatial variation when a sea-level rise was imposed (Figure 9), consistent with the expectation of further drowning. As a further test of this notion, an equally large

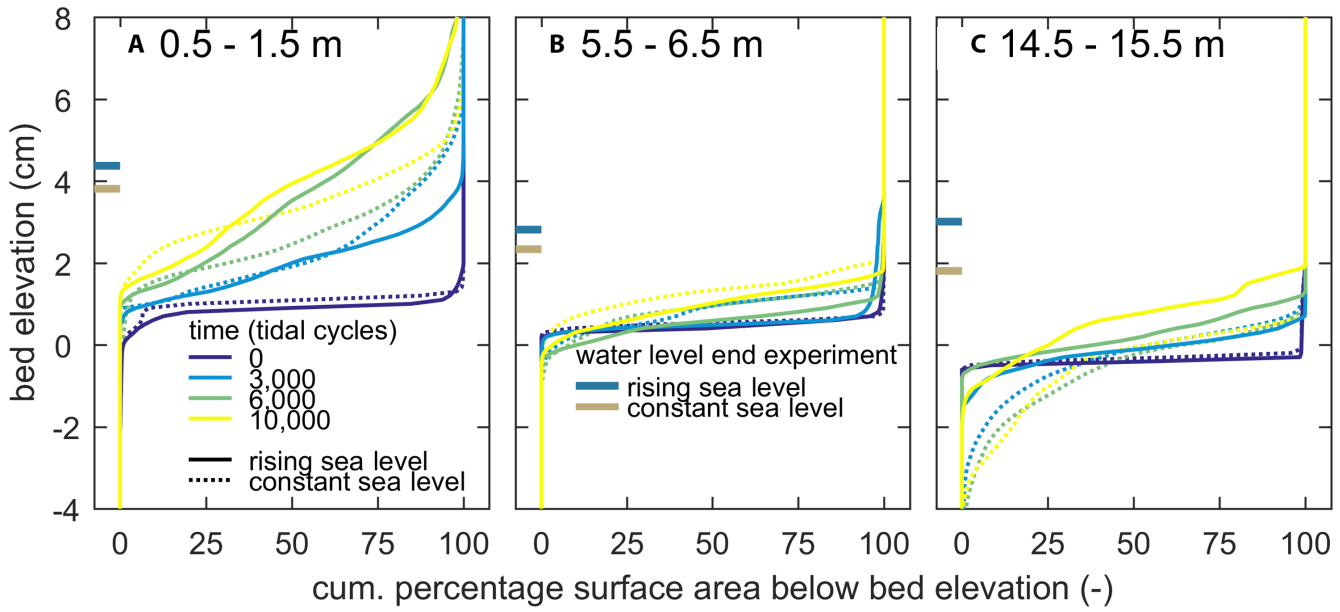

FIGURE 6 Development of cumulative bed elevation distribution for the experiment with constant sea level and the experiment with rising sea level (A) for the bay-head delta, (B) the drowned bay and (C) the downstream part of the flood-tidal delta. The bed elevation profiles exclude the unreworked outer banks along the estuary and include the valley slope. Mean water levels are given for the final time step at 10,000 cycles and derived from numerical modelling in Nays2D. The high bed elevation on the bay-head delta explains the relatively high water level at the upstream part of the estuary in (A).

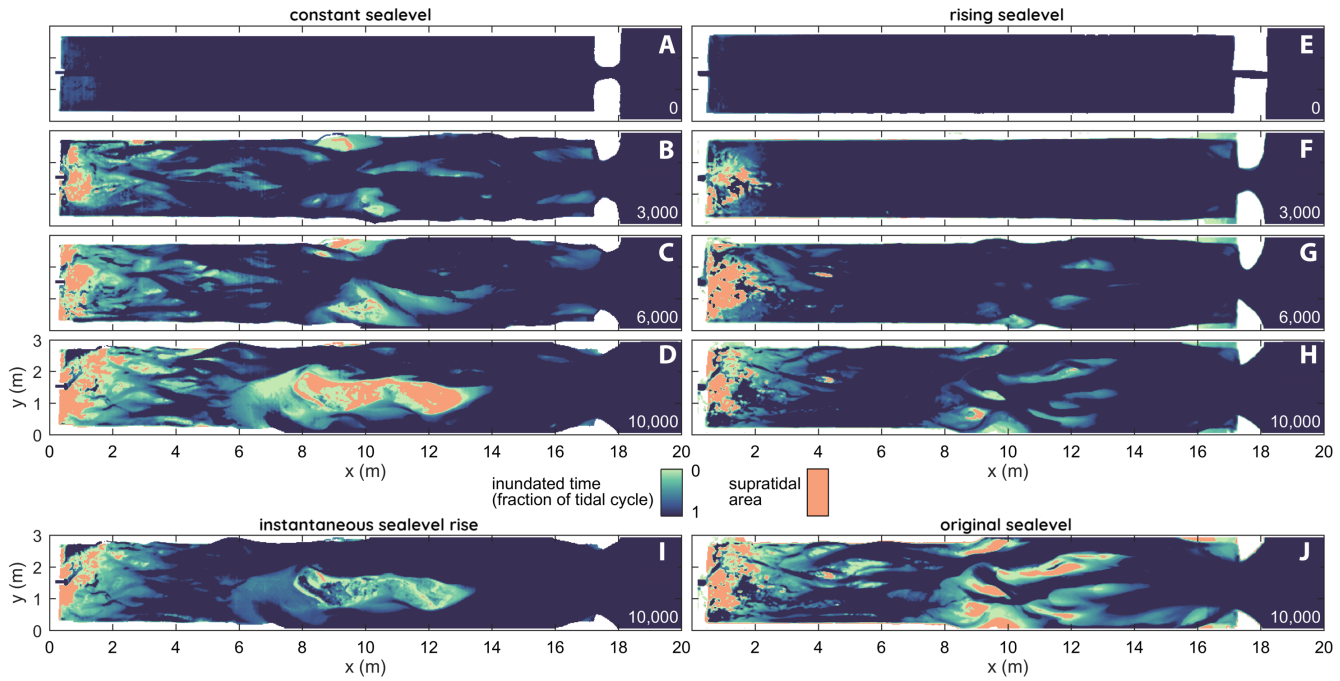

FIGURE 7 Maps of inundation duration normalised by the tidal period for the experiment with constant sea level (left column) and the experiment with sea-level rise (right column). Panel I shows the inundation duration if an instantaneous 7 mm sea-level rise was imposed on the final time step of the experiment with constant sea level. Panel J shows the inundation duration for the final time step of the experiment with sea-level rise if the original sea level is imposed (i.e. an instantaneous 7 mm sea-level lowering).

but instantaneous sea-level rise was imposed in the numerical model on the final bathymetry of the estuary experiment with constant sea level. This resulted in so much deepening that supratidal area nearly disappeared and intertidal area was much reduced (Figure 9I). Likewise, numerically modelling flow, without sea-level rise imposed on the final bathymetry of the experiment with sea-level rise, shows a considerable increase of intertidal and

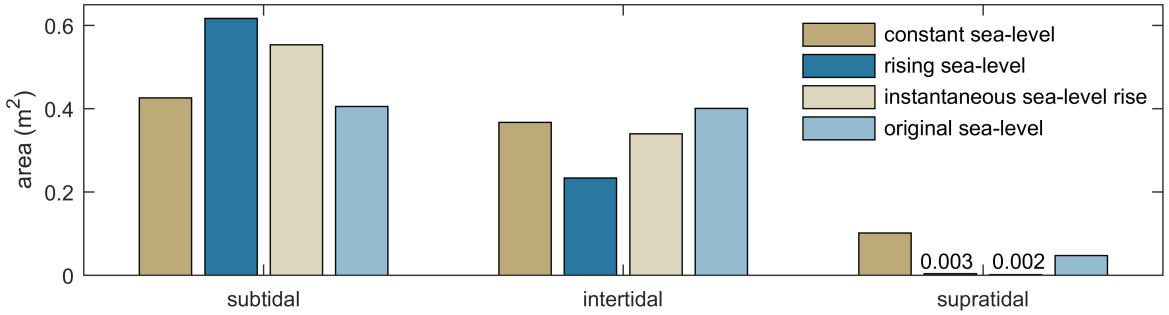

FIGURE 8 Effect of sea-level rise on subtidal, intertidal and supratidal area for the reach $x = 6–14$ m, plotted for the final time step of the constant sea level and the rising sea-level experiments. Also, the hypothetical distribution of the tidal zones are given for the constant sea-level experiment with instantaneous sea-level rise, and for the rising sea-level experiment with its original sea level to cross-reference their development. Unreworked floodplains at the estuary banks are not included in the area calculation.

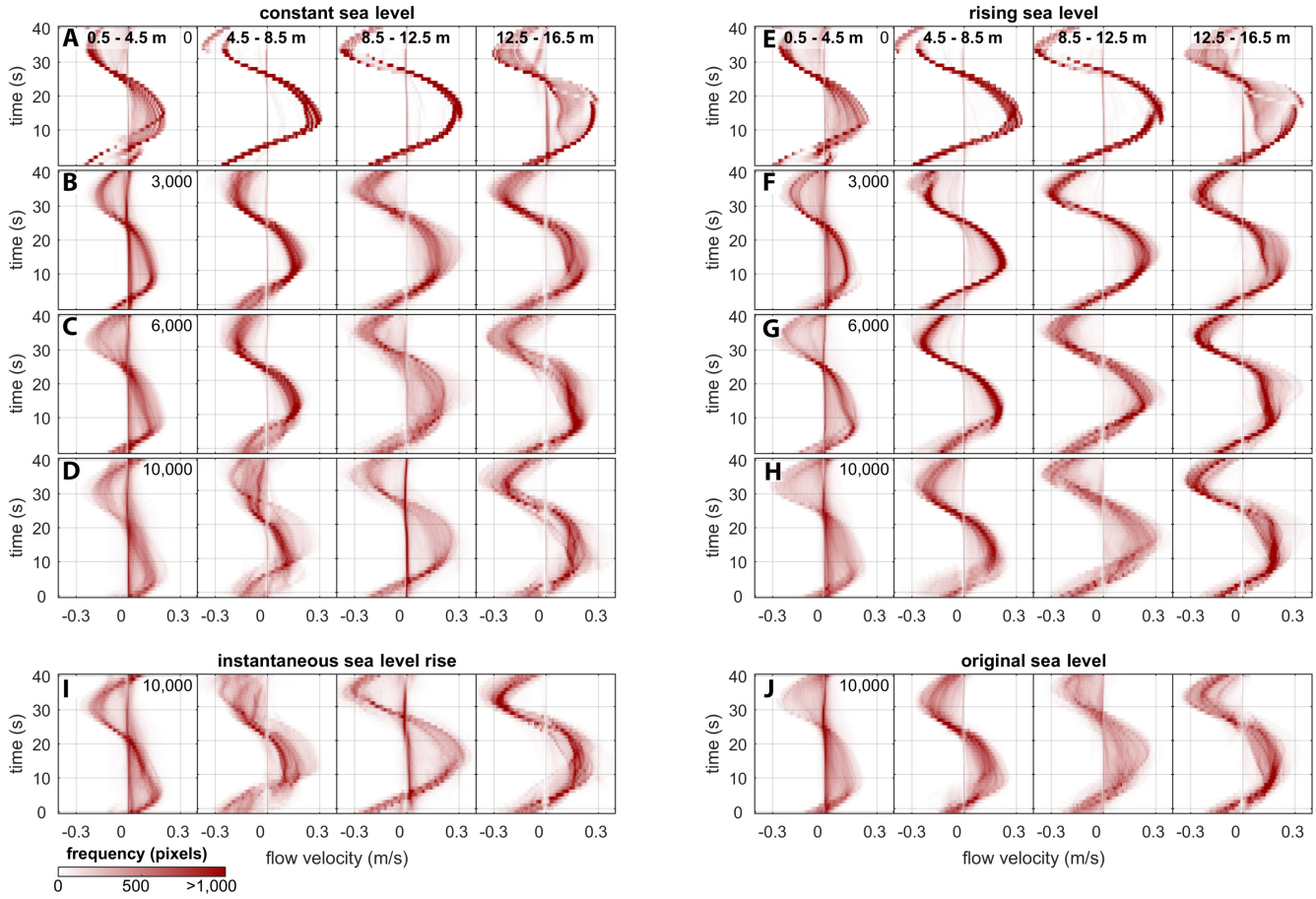

FIGURE 9 Distributions of flow velocity over time in four reaches along the estuary. Panel I shows the flow velocities if an instantaneous 7 mm sea-level rise was imposed on the final time step of the experiment with constant sea level. Panel J shows the flow velocities for the final time step of the experiment with sea-level rise if the original sea level is imposed (i.e. an instantaneous 7 mm sea-level lowering).

supratidal area along the entire estuary. The occurrence of larger flow velocities under sea-level rise points at reduced friction mainly due to greater water depths. Additionally, morphological complexity influenced the flow pattern, as the abundant intertidal and supratidal areas in the constant sea-level experiment (Figure 7A through D) resulted in much more spatial variation in flow velocity than in the sea-level rise experiment (Figure 7E through H). This was particularly clear for the subtidal bay in the range $x = 4.5–8.5$ m (Figure 9E through H).

4 | DISCUSSION

The net importing estuary experiment showed that imported marine sediment was deposited closer to its coastal source under sea-level rise conditions compared to a control experiment with constant sea level (Weisscher et al., 2022). Such deposition progressively closer to its marine source resembles the back-stepping seen on river deltas under sea-level rise, but here in the reverse direction: not back-stepping upstream, but retreating downstream towards the coastal sediment source. As a result, the central estuary between the bay-head delta and flood-tidal delta drowned, and vegetation was mostly limited to the bay-head delta. Below, the trends in the experiments are compared with models and observations in various environments and implications are inferred for estuarine responses to future sea-level rise.

4.1 | Estuary drowning

The experiment showed that sea-level rise influenced the locations for sediment deposition along an estuary (Figures 3 and 5). More specifically, the bay-head delta and flood-tidal delta continued to receive sediment from the nearby fluvial and marine sources, whilst the middle-to-upstream reach of the estuary experienced sediment starvation and deepened (Figure 7). Under a constant sea level, the development of bars was limited by water depth as shallower flow led to reduced sediment mobility and less vertical accretion. Hence, any additional imported sediment was transported further upstream to drive land-level rise along the entire estuary. This limitation by water depth was also found for braided sand-bed rivers, in which bar complexes are predominantly formed by lateral channel migration in scale experiments (Schuurman et al., 2013; Van de et al., 2013). However, braided rivers have ample sediment and about constant discharge for a given reach, whilst the experimental estuaries started unfilled and had an upstream decreasing tidal prism. Therefore, vertical accretion in the middle estuary was also in part limited by sediment availability, especially so in the sea-level rise experiment where accommodation increased over time. Both the bay-head delta and the flood-tidal delta showed mild back-stepping under sea-level rise, caused by sediment deposition progressively closer to the sources of the river and the tidal inlet. This resulted not only in higher bed elevations at the bay-head delta and flood-tidal delta (Figures 5 and 6A,C), but also in a clear disconnect between the fluvial and marine sediments in the middle estuary, which then drowned. This disconnect probably also explains why the subtidal channels did not collectively converge in the upstream direction like in the constant sea-level experiment (Figures 7 and 10; Weisscher et al., 2022).

Sea-level rise negated the eco-engineering effect of the vegetation and limited the area suitable for vegetation

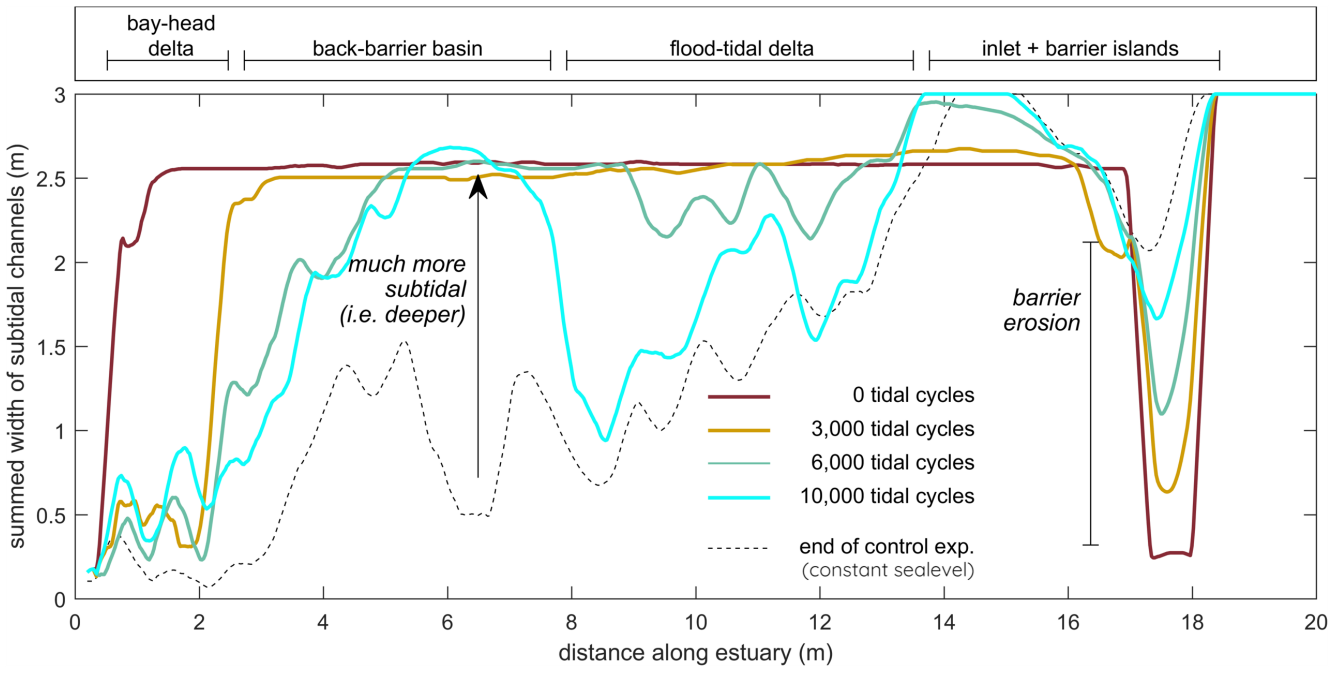

FIGURE 10 Summed width of subtidal area, showing the development of bay-head delta and flood-tidal delta as the barriers erode. Compared with the control experiment with a constant sea level, the central-to-upstream reach of the estuary remains subtidal throughout the sea-level rise experiment, indicative of insufficient sediment import to keep up with sea-level rise.

establishment. Accordingly, vegetated bars remained small, typically had a shorter lifespan and were separated by subtidal channels. Although the number of *Lotus* and *Veronica* patches was larger under sea-level rise conditions, their collective abundance within the estuary was considerably smaller. Hence, the patches proved less effective at focussing tidal flow and increasing upstream sediment transport as seen in the constant sea-level experiment. The patches promoted mud deposition at their rims and foreshores, yet neither mud nor vegetation was necessary for the settling of the other, conforming to field data (Van der et al., 2008) and numerical modelling (Brückner et al., 2019). This deposition pattern is similar to natural salt marshes (Schwarz et al., 2018; Vandenbruwaene et al., 2015), where mud deposition may quickly reduce flow onto the salt marsh, which sometimes results in topographical lows bounded by narrow levees (Best et al., 2018; Boechat Albernaz et al., 2020). In nature, such a morphology is likely more prone to quick removal of vegetation by a rising sea level and may also contribute to less suitable areas for vegetation establishment after drowning (Mariotti & Fagherazzi, 2010).

Flow velocities increased and became more spatially uniform as the estuary deepened under sea-level rise. Such spatial uniformity is also found in natural unfilled estuaries, where tidal flow velocity generally decreases upon entering a wide and deep subtidal bay from the sea (Dalrymple et al., 1992; Roy et al., 1980). In nature, tidal prism decreases in the upstream direction, but in a tilting flume it can also increase (Kleinhans et al., 2017b). In both ingressive and infilling experimental estuaries, the tidal prism quickly develops an upstream decreasing trend (compare Braat et al., 2019 and Weisscher et al., 2022). However, in the experiment with sea-level rise, the filling of accommodation could not keep up and, as a result, the tidal action and morphodynamics (due to tilting the flume) may have been larger in the subtidal bay than expected in nature. Furthermore, the flood-tidal delta and the bay-head delta tended to back-step towards their respective sediment source, which seems unlikely to be caused by slightly larger tidal currents in the subtidal bay where the flow is much deeper than on the deltas. The new experiment indicates that also a flood-tidal delta may undergo a form of back-stepping or retreat closer to its source of marine sediment upon relative sea-level rise (Figure 5). This retreat did not show the distinct lobes that deltas form, which may relate to the tidal currents over the flood-tidal delta.

Experimental estuary deepening in response to sea-level rise resembles palaeogeographical reconstruction cases of coastal drowning in the Early Holocene (Allen & Posamentier, 1993; Vos, 2015). An example that became progressively more unfilled in response to sea-level rise is the Gironde River valley during the Middle Holocene (Allen & Posamentier, 1993; Dalrymple et al., 1992). This system showed a clear disconnect between the marine flood-tidal delta and the more fluvial bay-head delta, with few intertidal flats and salt marshes bordering the subtidal bay. Nonetheless, the deep subtidal bay of the Gironde Estuary was largely muddy, which differs from the generally sandy subtidal bay in the experiments. This difference is likely due to a relatively smaller input of fines into the inlet and into the river combined with the large trapping efficiency of the vegetated bay-head delta in the experiment. Since the sea-level rise experiment was mainly shaped by tides and waves and only a little by the river, a more significant fluvial influence would probably result in a larger sediment flux towards the central estuary and slower drowning.

The experimental estuary was set in an initially wide drowned valley, which may respond differently to sea-level rise than confined estuaries. In wide drowned valleys, the erosive power of the tidal flow drastically reduces upon entering the estuary, which implies that estuary filling largely depends on fluvial and marine sediment input (Roy et al., 1980) and expanding salt marshes (Beets & Van der Spek, 2000; De Haas et al., 2018). Conversely, the funnel-like shape of confined estuaries leads to strong flow velocities along an estuary. Therefore, estuary reaches that face sediment starvation are hypothesised to experience outer bank erosion to elevate bars and channels if fluvial and marine sediment supply is insufficient (Leuven et al., 2019). More work is needed to address this issue of potential outer bank erosion.

4.2 | Flood-tidal delta aggradation and retreat

The sea-level rise experiment shows higher aggradation and reduced expansion into the estuary compared to the constant sea-level experiment. Simultaneously, the bay-head delta also faces higher aggradation that is focussed closer to the upstream boundary. So, both deltas migrate towards their respective sediment sources, which are at opposite ends of the estuary. Such retreating deltas are also observed in experimental studies of fluvial deltas with sea-level rise (Guerit et al., 2021; Muto & Steel, 2001). There, the back-stepping of delta lobes is attributed to avulsions instead of allogenic changes in sediment supply or accommodation creation. Conversely, the experiments in this study suggest that sea-level rise influences delta retreat as well. These different findings may be related to the aspect ratios of the experiments: in the Metronome, morphological change is most prominent along the longitudinal axis, whereas Muto and Steel (2001) created an experiment

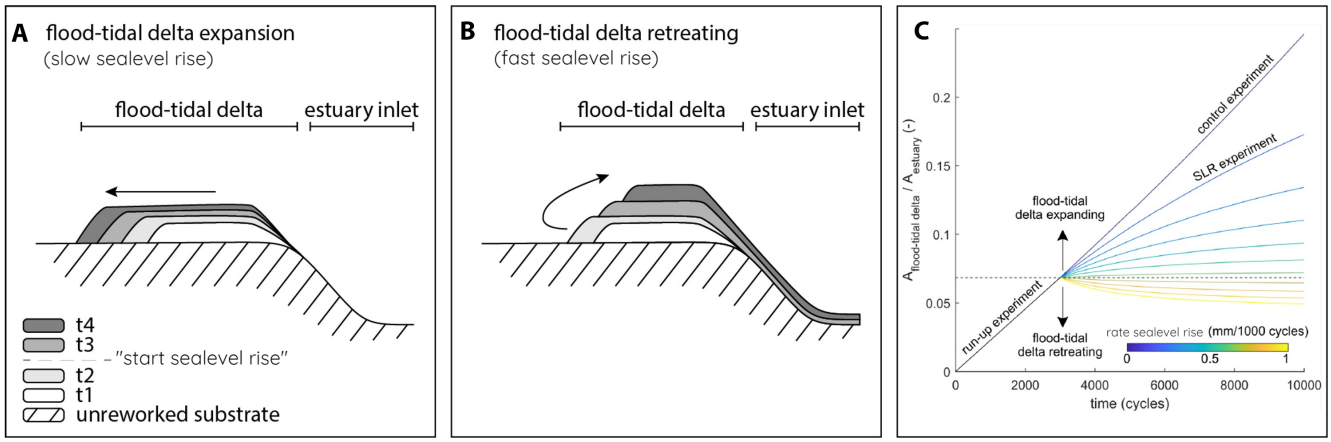

FIGURE 11 Conceptual hypothesised development of a flood-tidal delta under different sea-level rise scenarios. (A) Continued expansion of the flood-tidal delta under absent or mild sea-level rise. (B) Retreat of the flood-tidal delta upon fast sea-level rise. (C) Development of the flood-tidal delta extent under 10 different sea-level rise scenarios, of which two were tested and presented in this study.

with more room for avulsions and compensational stacking in the dimension perpendicular to the mean flow. It was not feasible to generate the avulsions, which are the controlling back-stepping mechanism according to Muto and Steel (2001), in a similar fashion in the Metronome due to the lateral boundaries of the experiment.

Back-stepping of para-sequences during a transgressive phase of a sea-level cycle is well-known in sequence stratigraphy literature (Catuneanu et al., 2009) but not so much for flood-tidal deltas. The relationship between the rate of sea-level rise and the development of a flood-tidal delta is explored in Figure 11. Figure 11C shows the extent of a flood-tidal delta in the experimental setup under different hypothetical rates of sea-level rise but otherwise subject to the same conditions (e.g. assumed constant sediment supply by barrier erosion). This conceptualisation shows that there is a tipping point from flood-tidal delta expansion (Figure 11A) to retreat (Figure 11B) with increasing sea-level rise. Combined with observations of longitudinal bedlevel change (Figure 5), this leads to the hypothesis that fast sea-level rise can result in the downstream retreat of a flood-tidal delta (i.e. towards the sea).

5 | CONCLUSION

Rapid sea-level rise causes imported sediment deposition closer to its marine and fluvial sources in scale experiments of infilling estuaries. Sea-level rise created additional accommodation, but insufficient sediment was transported beyond the river-fed bay-head delta and eroded from the coastal barriers to fill all accommodation despite an increased tidal discharge due to sea-level rise. Consequently, intertidal and supratidal areas mostly drowned in the central reach of the estuary. Locally, vegetation stabilised bars and facilitated vertical accretion, but sea-level rise compromised the eco-engineering effects of vegetation by longer inundation times and increased channel migration. Mud was mostly deposited on the bay-head delta and the declining intertidal flats. The hypothesis of a landward shift of depositional units was not observed in the sea-level rise experiment. Instead, sea-level rise caused sediment to be supplied closer to its fluvial and marine sources, which resulted in the bay-head delta and flood-tidal delta keeping up with sea-level rise. Therefore, the central reach of the estuary received insufficient sediment to compensate for the newly created accommodation by sea-level rise and drowned. This suggests that keeping pace with sea-level rise not only depends on the sea-level rise rate, but also on the length of a tidal system and antecedent conditions such as river valley width.

ACKNOWLEDGEMENTS

The authors thank A. W. Martinius and two anonymous for their insightful comments that helped improve the manuscript. The new experiment was conducted by Pelle H. Adema for his MSc thesis with help by assistant Jan-Eike Rossius and by Steven A. H. Weisscher as part of his PhD research. This research was supported by the European Research Council (ERC Consolidator grant 647570 to Maarten G. Kleinhans). The authors state there was no conflict of interest. The authors contributed in the following proportions to conception and design, conducting experiments, analysis and conclusions, and manuscript preparation: SAHW(40,10,40,40%), PHA(20,50,40,40%), JER (0,40,0,0%) and MGK(40,0,20,20%).

DATA AVAILABILITY STATEMENT

Data will be made available upon acceptance of the manuscript, including the DEMs, imagery and the input and output files of the hydrodynamic modelling in Nays2D.

ORCID

Steven A. H. Weisscher https://orcid.org/0000-0003-0238-2383
Pelle H. Adema https://orcid.org/0000-0001-5983-6943
Maarten G. Kleinhans https://orcid.org/0000-0002-9484-1673

REFERENCES

Allard, J., Chaumillon, E. & Féniès, H. (2009) A synthesis of morphological evolutions and Holocene stratigraphy of a wave-dominated estuary: the Arcachon lagoon, SW France. *Continental Shelf Research*, 29(8), 957–969.

Allen, G.P. & Posamentier, H.W. (1993) Sequence stratigraphy and facies model of an incised valley fill: the gironde estuary, France. *Journal of Sedimentary Research*, 63(3), 378–391.

Baar, A.W., Boechat-Albernaz, M., Van Dijk, W.M. & Kleinhans, M.G. (2019) Critical dependence of morpho-dynamic models of fluvial and tidal systems on empirical downslope sediment transport. *Nature Communications*, 10(1), 1–12.

Baumgardner, S. (2016) Quantifying Galloway: fluvial, tidal and wave influence on experimental and field deltas.

Beets, D.J. & Van der Spek, A.J.F. (2000) The Holocene evolution of the barrier and the back-barrier basins of Belgium and The Netherlands as a function of late Weichselian morphology, relative sea-level rise and sediment supply. *Netherlands Journal of Geosciences*, 79(1), 3–16.

Best, Ü.S.N., Van der Wegen, M., Dijkstra, J., Willemsen, P.W.J.M., Borsje, B.W. & Roelvink, D.J.A. (2018) Do salt marshes survive sea level rise? modelling wave action, morphodynamics and vegetation dynamics. *Environmental Modelling & Software*, 109, 152–166.

Boechat Albernaz, M., Roelofs, L., Pierik, H.J. & Kleinhans, M.G. (2020) Natural levee evolution in vegetated fluvial-tidal environments. *Earth Surface Processes and Landforms*, 45(15), 3824–3841.

Bokulich, A. & Oreskes, N. (2017) Models in Geosciences. In: Magnani, L. & Bertolotti, T. (Eds.) *Springer Handbook of Model-Based Science*. Cham: Springer. https://doi.org/10.1007/978-3-319-30526-4_41

Braat, L., Leuven, J.R.F.W., Lokhorst, I.R. & Kleinhans, M.G. (2019) Effects of estuarine mudflat formation on tidal prism and large-scale morphology in experiments. *Earth Surface Processes and Landforms*, 44(2), 417–432.

Braat, L., Van Kessel, T., Leuven, J.R.F.W. & Kleinhans, M.G. (2017) Effects of mud supply on large-scale estuary morphology and development over centuries to millennia. *Earth Surface Dynamics*, 5(4), 617–652.

Brückner, M.Z.M., Mcmahon, W.J. & Kleinhans, M.G. (2021) Muddying the waters: modeling the effects of early land plants in paleozoic estuaries. *Palaios*, 36(5), 173–181.

Brückner, M.Z.M., Schwarz, C., Van Dijk, W.M., Van Oorschot, M., Douma, H. & Kleinhans, M.G. (2019) Salt marsh establishment and eco-engineering effects in dynamic estuaries determined by species growth and mortality. *Journal of Geophysical Research: Earth Surface*, 124(12), 2962–2986.

Catuneanu, O., Abreu, V., Bhattacharya, J.P., Blum, M.D., Dalrymple, R.W., Eriksson, P.G., Fielding, C.R., Fisher, W.L., Galloway, W.E., Gibling, M.R., Giles, K.A., Holbrook, J.M., Jordan, R., Kendall, C.G.S.C., Macurda, B., Martinsen, O.J., Miall, A.D., Neal, J.E., Nummedal, D., Pomar, L., Posamentier, H.W., Pratt, B.R., Sarg, J.F., Shanley, K.W., Steel, R.J., Strasser, A., Tucker, M.E. & Winker, C. (2009) Towards the standardization of sequence stratigraphy. *Earth-Science Reviews*, 92(1–2), 1–33.

Clement, A.J.H., Fuller, I.C. & Sloss, C.R. (2017) Facies architecture, morphostratigraphy, and sedimentary evolution of a rapidly-infilled Holocene incised-valley estuary: the lower Manawatu valley, North Island New Zealand. *Marine Geology*, 390, 214–233.

Cotton, J.A., Wharton, G., Bass, J.A.B., Heppell, C.M. & Wotton, R.S. (2006) The effects of seasonal changes to in-stream vegetation cover on patterns of flow and accumulation of sediment. *Geomorphology*, 77(3–4), 320–334.

Dalrymple, R.W. & Choi, K. (2007) Morphologic and facies trends through the fluvial–marine transition in tide-dominated depositional systems: a schematic framework for environmental and sequence-stratigraphic interpretation. *Earth-Science Reviews*, 81(3–4), 135–174.

Dalrymple, R.W., Zaitlin, B.A. & Boyd, R. (1992) Estuarine facies models; conceptual basis and stratigraphic implications. *Journal of Sedimentary Research*, 62(6), 1130–1146.

De Haas, T., Pierik, H.-J., Van der Spek, A.J.F., Cohen, K.M., Van Maanen, B. & Kleinhans, M.G. (2018) Holocene evolution of tidal systems in The Netherlands: effects of rivers, coastal boundary conditions, eco-engineering species, inherited relief and human interference. *Earth-Science Reviews*, 177, 139–163.

De Haas, T., Van der Valk, L., Cohen, K.M., Pierik, H.-J., Weisscher, S.A.H., Hijma, M.P., Van der Spek, A.J.F. & Kleinhans, M.G. (2019) Long-term evolution of the Old Rhine estuary: unravelling effects of changing boundary conditions and inherited landscape. *The Depositional Record*, 5(1), 84–108.

Du, J., Shen, J., Zhang, Y.J., Ye, F., Liu, Z., Wang, Z., Wang, Y.P., Yu, X., Sisson, M. & Wang, H.V. (2018) Tidal response to sea-level rise in different types of estuaries: the importance of length, bathymetry, and geometry. *Geophysical Research Letters*, 45(1), 227–235.

Elmilady, H.M.S.M.A., Van der Wegen, M., Roelvink, D. & Van der Spek, A. (2020) Morphodynamic evolution of a fringing sandy shoal: from tidal levees to sea level rise. *Journal of Geophysical Research: Earth Surface*, 125(6), e2019JF005397.

Elmilady, H.M.S.M.A., Van der Wegen, M., Roelvink, D. & Van der Spek, A. (2022) Modeling the morphodynamic response of estuarine intertidal shoals to sea-level rise. *Journal of Geophysical Research: Earth Surface*, 127(1), e2021JF006152.

Féniès, H. & Faugères, J.-C. (1998) Facies and geometry of tidal channel-fill deposits (Arcachon Lagoon, SW France). *Marine Geology*, 150(1–4), 131–148.

Friedrichs, C.T. (1995) Stability shear stress and equilibrium cross-sectional geometry of sheltered tidal channels. *Journal of Coastal Research*, 11(4), 1062–1074.

Friedrichs, C.T. & Aubrey, D.G. (1988) Non-linear tidal distortion in shallow well-mixed estuaries: a synthesis. *Estuarine, Coastal and Shelf Science*, 27(5), 521–545.

Guerit, L., Foreman, B., Chen, C., Paola, C. & Castelltort, S. (2021) Autogenic delta progradation during sea-level rise within incised valleys. *Geology*, 49(3), 273–277.

Guo, L., Xu, F., Van der Wegen, M., Townend, I., Wang, Z.B. & He, Q. (2021) Morphodynamic adaptation of a tidal basin to

centennial sea-level rise: the importance of lateral expansion. *Continental Shelf Research*, 226, 104494.

Guo, L., Zhu, C., Xu, F., Xie, W., Van der Wegen, M., Townend, I., Wang, Z.B. & He, Q. (2022) Reclamation of tidal flats within tidal basins alters centennial morphodynamic adaptation to sea-level rise. *Journal of Geophysical Research: Earth Surface*, 127(6), e2021JF006556.

Hijma, M.P. & Cohen, K.M. (2010) Timing and magnitude of the sea-level jump preluding the 8200 yr event. *Geology*, 38(3), 275–278.

Job, T., Penny, D., Morgan, B., Hua, Q., Gadd, P. & Zawadzki, A. (2021) Multi-stage holocene evolution of the river murray estuary, South Australia. *The Holocene*, 31(1), 50–65.

Kleinhans, M.G., Leuven, J.R.F.W., Braat, L. & Baar, A.W. (2017) Scour holes and ripples occur below the hydraulic smooth to rough transition of movable beds. *Sedimentology*, 64(5), 1381–1401.

Kleinhans, M.G., Roelofs, L., Weisscher, S.A.H., Lokhorst, I.R. & Braat, L. (2022) Estuarine morphodynamics and development modified by floodplain formation. *Earth Surface Dynamics*, 10(2), 367–381.

Kleinhans, M.G., Van Der Vegt, M., Leuven, J.R.F.W., Braat, L., Markies, H., Simmelink, A., Roosendaal, C., Van Eijk, A., Vrijbergen, P. & Van Maarseveen, M. (2017) Turning the tide: comparison of tidal flow by periodic sea level fluctuation and by periodic bed tilting in scaled landscape experiments of estuaries. *Earth Surface Dynamics*, 5(4), 731–756.

Kleinhans, M.G., Van Dijk, W.M., Van de Lageweg, W.I., Hoyal, D.C.J.D., Markies, H., Van Maarseveen, M., Roosendaal, C., Van Weesep, W., Van Breemen, D., Hoendervoogt, R. & Cheshier, N. (2014) Quantifiable effectiveness of experimental scaling of river- and delta morphodynamics and stratigraphy. *Earth-Science Reviews*, 133, 43–61.

Kleinhans, M.G., Van Rosmalen, T.M., Roosendaal, C. & Van der Vegt, M. (2014) Turning the tide: mutually evasive ebb-and flood-dominant channels and bars in an experimental estuary. *Advances in Geosciences*, 39, 21–26.

Kleinhans, M.G., Van Scheltinga, R.T., Van Der Vegt, M. & Markies, H. (2015) Turning the tide: growth and dynamics of a tidal basin and inlet in experiments. *Journal of Geophysical Research: Earth Surface*, 120(1), 95–119.

Lanzoni, S. & Seminara, G. (2002) Long-term evolution and morphodynamic equilibrium of tidal channels. *Journal of Geophysical Research: Oceans*, 107(C1), 1–13.

Leuven, J.R.F.W., Braat, L., Van Dijk, W.M., De Haas, T., Van Onselen, E.P., Ruessink, B.G. & Kleinhans, M.G. (2018) Growing forced bars determine nonideal estuary planform. *Journal of Geophysical Research: Earth Surface*, 123(11), 2971–2992.

Leuven, J.R.F.W., De Haas, T., Braat, L. & Kleinhans, M.G. (2018) Topographic forcing of tidal sandbar patterns for irregular estuary planforms. *Earth Surface Processes and Landforms*, 43(1), 172–186.

Leuven, J.R.F.W., Pierik, H.-J., Van der Vegt, M., Bouma, T.J. & Kleinhans, M.G. (2019) Sea-level-rise-induced threats depend on the size of tide-influenced estuaries worldwide. *Nature Climate Change*, 9(12), 986–992.

Lokhorst, I.R., De Lange, S.I., Van Buiten, G., Selaković, S. & Kleinhans, M.G. (2019) Species selection and assessment of eco-engineering effects of seedlings for biogeomorphological landscape experiments. *Earth Surface Processes and Landforms*, 44(14), 2922–2935.

Luhar, M., Rominger, J. & Nepf, H. (2008) Interaction between flow, transport and vegetation spatial structure. *Environmental Fluid Mechanics*, 8(5), 423–439.

Mariotti, G. & Fagherazzi, S. (2010) A numerical model for the coupled long-term evolution of salt marshes and tidal flats. *Journal of Geophysical Research: Earth Surface*, 115(F1), 1–5.

Moore, R.D., Wolf, J., Souza, A.J. & Flint, S.S. (2009) Morphological evolution of the Dee Estuary, Eastern Irish Sea, UK: a tidal asymmetry approach. *Geomorphology*, 103(4), 588–596.

Muto, T. & Steel, R.J. (2001) Autostepping during the transgressive growth of deltas: results from flume experiments. *Geology*, 29(9), 771–774.

Nichol, S.L. (1991) Zonation and sedimentology of estuarine facies in an incised valley, wave-dominated, microtidal setting, New South Wales, Australia. In: *Tidal sedimentology*. Calgery, Alberta: CSPG Special Publications, pp. 41–58.

O'Brien, M.P. (1969) Equilibrium flow areas of inlets on sandy coasts. *Journal of the Waterways and Harbors Division*, 95(1), 43–52.

Oreskes, N., Shrader-Frechette, K. & Belitz, K. (1994) Verification, validation, and confirmation of numerical models in the earth sciences. *Science*, 263(5147), 641–646.

Pierik, H.-J. (2021) Landscape changes and human–landscape interaction during the first millennium AD in The Netherlands. *Netherlands Journal of Geosciences*, 100(e11), 1–14.

Reynolds, O. (1889). Report of the committee appointed to investigate the action of waves and currents on the beds and foreshores of estuaries by means of working models, British Association Report. Papers on mechanical and physical subjects, 2:380–481.

Roep, T. & Van Regteren Altena, J. (1988) 1988: Paleotidal levels in tidal sediments (3800–3635 BP); compaction, sea level rise and human occupation (3275–2620 BP) at Bovenskarpel, NW Netherlands. In: de Boer, P.L., van Gelder, A. & Nio, S.D. (Eds.) *Tide-influenced sedimentary environments and facies*. Dordrecht: Reidel, pp. 215–231.

Roy, P.S., Thom, B.G. & Wright, L.D. (1980) Holocene sequences on an embayed high-energy coast: an evolutionary model. *Sedimentary Geology*, 26(1–3), 1–19.

Schuurman, F., Marra, W.A. & Kleinhans, M.G. (2013) Physics-based modeling of large braided sand-bed rivers: bar pattern formation, dynamics, and sensitivity. *Journal of Geophysical Research: Earth Surface*, 118(4), 2509–2527.

Schwarz, C., Gourgue, O., Van Belzen, J., Zhu, Z., Bouma, T.J., Van De Koppel, J., Ruessink, G., Claude, N. & Temmerman, S. (2018) Self-organization of a biogeomorphic landscape controlled by plant life-history traits. *Nature Geoscience*, 11(9), 672–677.

Shi, Z. & Lamb, H.F. (1991) Post-glacial sedimentary evolution of a microtidal estuary, Dyfi Estuary, West Wales, U.K. *Sedimentary Geology*, 73(3–4), 227–246.

Shimizu, Y., Kobatake, S. & Arafune, T. (2000) Numerical study on the flood-flow stage in gravel-bed river with the excessive reverine trees. *Proceedings of Hydraulic Engineering*, 44, 819–824 (in Japanese).

Simon, A. & Collinson, A.J. (2002) Quantifying the mechanical and hydrologic effects of riparian vegetation on streambank stability. *Earth Surface Processes and Landforms*, 27(5), 527–546.

Stefanon, L., Carniello, L., D'Alpaos, A. & Lanzoni, S. (2010) Experimental analysis of tidal network growth and development. *Continental Shelf Research*, 30(8), 950–962.

Stefanon, L., Carniello, L., D'Alpaos, A. & Rinaldo, A. (2012) Signatures of sea level changes on tidal geomorphology: experiments on network incision and retreat. *Geophysical Research Letters*, 39(12), 1–6.

Stella, J.C., Hayden, M.K., Battles, J.J., Piégay, H., Dufour, S. & Fremier, A.K. (2011) The role of abandoned channels as refugia for sustaining pioneer riparian forest ecosystems. *Ecosystems*, 14(5), 776–790.

Tal, M. & Paola, C. (2007) Dynamic single-thread channels maintained by the interaction of flow and vegetation. *Geology*, 35(4), 347–350.

Van de Lageweg, W.I., Van Dijk, W.M. & Kleinhans, M.G. (2013) Channel belt architecture formed by a meandering river. *Sedimentology*, 60(3), 840–859.

Van der Spek, A.J.F. & Beets, D.J. (1992) Mid-holocene evolution of a tidal basin in the western Netherlands: a model for future changes in the northern Netherlands under conditions of accelerated sea-level rise? *Sedimentary Geology*, 80(3–4), 185–197.

Van der Wal, D., Herman, P.M.J., Forster, R.M., Ysebaert, T., Rossi, F., Knaeps, E., Plancke, Y.M.G. & Ides, S.J. (2008) Distribution and dynamics of intertidal macrobenthos predicted from remote sensing: response to microphytobenthos and environment. *Marine Ecology Progress Series*, 367, 57–72.

Van der Molen, J. & De Swart, H. (2001) Holocene tidal conditions and tide-induced sand transport in the southern north sea. *Journal of Geophysical Research: Oceans*, 106(C5), 9339–9362.

van der Wegen, M. (2013) Numerical modeling of the impact of sea level rise on tidal basin morphodynamics. *Journal of Geophysical Research: Earth Surface*, 118(2), 447–460.

Van Dijk, W.M., Cox, J.R., Leuven, J.R.F.W., Cleveringa, J., Taal, M., Hiatt, M.R., Sonke, W., Verbeek, K., Speckmann, B. & Kleinhans, M.G. (2021) The vulnerability of tidal flats and multi-channel estuaries to dredging and disposal. *Anthropocene Coasts*, 4(1), 36–60.

Van Maren, D.S., Oost, A.P., Wang, Z.B. & Vos, P.C. (2016) The effect of land reclamations and sediment extraction on the suspended sediment concentration in the Ems Estuary. *Marine Geology*, 376, 147–157.

Vandenbruwaene, W., Schwarz, C., Bouma, T.J., Meire, P. & Temmerman, S. (2015) Landscape-scale flow patterns over a vegetated tidal marsh and an unvegetated tidal flat: implications for the landform properties of the intertidal floodplain. *Geomorphology*, 231, 40–52.

Vos, P. (2015) *Origin of the Dutch coastal landscape: long-term landscape evolution of The Netherlands during the Holocene, described and visualized in national, regional and local palaeogeographical map series*. Groningen: Barkhuis.

Vos, P., Meulen, M., Weerts, H. & Bazelmans, J. (2018) Atlas van Nederland in het Holoceen. In: *Landschap en bewoning vanaf de laatste ijstijd tot nu*. Amsterdam: Prometheus.

Weisscher, S.A.H., Boechat Albernaz, M., Leuven, J.R.F.W., Van Dijk, W.M., Shimizu, Y. & Kleinhans, M.G. (2020) Complementing scale experiments of rivers and estuaries with numerically modelled hydrodynamics. *Earth Surface Dynamics*, 8(4), 955–972.

Weisscher, S.A.H., Van den Hoven, K., Pierik, H.-J. & Kleinhans, M.G. (2022) Building and raising land: mud and vegetation effects in infilling estuaries. *Journal of Geophysical Research: Earth Surface*, 127(1), 1–24.

Zong, L. & Nepf, H. (2011) Spatial distribution of deposition within a patch of vegetation. *Water Resources Research*, 47(3), W03516.

How to cite this article: Weisscher, S.A.H., Adema, P.H., Rossius, J.-E. & Kleinhans, M.G. (2023) The effect of sea-level rise on estuary filling in scaled landscape experiments. *The Depositional Record*, 9, 363–379. Available from: https://doi.org/10.1002/dep2.233